SCIENCE CHINA
Earth Sciences

• RESEARCH PAPER •

August 2014 Vol.57 No.8: 1834–1845
doi: 10.1007/s11430-014-4852-1

Distribution and changes of active layer thickness (ALT) and soil temperature (TTOP) in the source area of the Yellow River using the GIPL model

LUO DongLiang[1*], JIN HuiJun[1], Sergei MARCHENKO[1,2] & Vladimir ROMANOVSKY[2]

[1] *State Key Laboratory of Frozen Soils Engineering, Cold and Arid Regions Environmental and Engineering Research Institute, Chinese Academy of Sciences, Lanzhou 730000, China;*
[2] *Geophysical Institute, University of Alaska Fairbanks, Fairbanks, Alaska 99775, USA*

Received October 2, 2013; accepted March 3, 2014; published online May 20, 2014

Active layer thickness (ALT) is critical to the understanding of the surface energy balance, hydrological cycles, plant growth, and cold region engineering projects in permafrost regions. The temperature at the bottom of the active layer, a boundary layer between the equilibrium thermal state (in permafrost below) and transient thermal state (in the atmosphere and surface canopies above), is an important parameter to reflect the existence and thermal stability of permafrost. In this study, the Geophysical Institute Permafrost Model (GIPL) was used to model the spatial distribution of and changes in ALT and soil temperature in the Source Area of the Yellow River (SAYR), where continuous, discontinuous, and sporadic permafrost coexists with seasonally frozen ground. Monthly air temperatures downscaled from the CRU TS3.0 datasets, monthly snow depth derived from the passive microwave remote-sensing data SMMR and SSM/I, and vegetation patterns and soil properties at scale of 1 : 1000000 were used as input data after modified with GIS techniques. The model validation was carried out carefully with in-situ ALT in the SAYR interpolated from the field-measured soil temperature data. The results of the model indicate that the average ALT in the SAYR has significantly increased from 1.8 m in 1980 to 2.4 m in 2006 at an average rate of 2.2 cm yr^{-1}. The mean annual temperature at the bottom of the active layer, or temperature at the top of permafrost (TTOP) rose substantially from –1.1°C in 1980 to –0.6°C in 2006 at an average rate of 0.018°C yr^{-1}. The increasing rate of the ALT and TTOP has accelerated since 2000. Regional warming and degradation of permafrost has also occurred, and the changes in the areal extent of regions with a sub-zero TTOP shrank from 2.4×10^4 to 2.2×10^4 km^2 at an average rate of 74 km^2 yr^{-1}. Changes of ALT and temperature have adversely affected the environmental stability in the SAYR.

GIPL model, active layer thickness, TTOP, degradation of permafrost

Citation: Luo D L, Jin H J, Marchenko S, et al. 2014. Distribution and changes of active layer thickness (ALT) and soil temperature (TTOP) in the source area of the Yellow River using the GIPL model. Science China: Earth Sciences, 57: 1834–1845, doi: 10.1007/s11430-014-4852-1

Permafrost is one of the key components in the cryosphere, and is very sensitive to climate changes and anthropogenic disturbances (Li et al., 2008). To improve the awareness and understanding of the ways in which permafrost is responding to climate change, many scientific projects on permafrost and active layer were conducted (e.g., Shiklomanov et al., 2008; Zhao et al., 2010). Among them, the most comprehensive and systematic study is the Circumpolar Active Layer Monitoring (CALM) program, which was designed for observing the temporal and spatial variability of the active layer and other near-surface permafrost parameters (Shiklomanov et al., 2008, 2010).

The active layer is usually defined as the top soil layer

*Corresponding author (email: luodongliang@lzb.ac.cn)

subject to seasonal freezing and thawing processes underlain by permafrost (van Everdingen, 2005). In some Russian and Chinese literature, the term also includes another distinct type: seasonally frozen layer overlying unfrozen ground inside or outside permafrost areas (van Everdingen, 2005; Zhou et al., 2000). The active layer plays significant roles in the global climate systems through its influences on surface energy exchanges, vegetation growth, hydrological cycles, and carbon budgets (Cheng and Wu, 2007; Guglielmin et al., 2008; Jin et al., 2008; Streletskiy et al., 2012; Wu et al., 2012). The temperature at bottom of the active layer, or the temperature at the top of permafrost (TTOP), can indicate the occurrence and thermal stability of permafrost (Sazonova and Romanovsky, 2003). Therefore, it is essential to study spatiotemporal variations of ALT and TTOP, which can help predict and assess the responses of environmental changes to climate warming.

There are many methods for calculating ALT and TTOP (e.g., Liu, 1983; Nelson and Outcalt, 1987; Pang et al., 2009). Perhaps the most widely used approach is the Stefan equation, which determines the ALT by calculating the square roots of thawing index (Romanovsky and Osterkamp, 1997; Zhang, 2005). However, studies by Romanovsky and Osterkamp (1997) indicated that simple Stefan equations present great systematic errors when applied at small spatial scales.

The Qinghai-Tibet Plateau (QTP), the so-called the Third Pole with an average elevation exceeding 4000 m above sea level (a.s.l.), responds sensitively to climate changes and anthropogenic activities because 70.6% of its areal extent is underlain by permafrost (Zhou et al., 2000), Of which more than half is warm permafrost (with temperature at depths of zero annual amplitude (MAGT) higher than −1°C) (Wu and Zhang, 2008). Therefore, this plateau permafrost is particularly vulnerable to climate changes. Accordingly, it has attracted increasingly more studies and investigations, such as those on the thermal and mechanical stability of soils in permafrost and the active layer, especially along the Qinghai-Tibet Highway and Railway (e.g. King et al., 2006; Cheng and Wu, 2007; Wu and Zhang, 2010; Li et al., 2012; Wu et al., 2012), also called the Qinghai-Tibet Engineering Corridor (QTEC) (Jin et al., 2008). However, those scattered and random observations are insufficient to illustrate variations in permafrost and active layer thicknesses and ground temperatures in the areas outside of the QTEC.

Permafrost models have the potential to overcome the shortages of the tedious field surveying and in-situ monitoring by setting up mathematical models and making use of a few accessible parameters such as elevation, air temperature, and ground surface temperatures (Riseborough et al., 2008; Pang et al., 2009; Guo et al., 2012). Cheng (1984) built a mathematical elevational model to simulate the distribution of elevational permafrost. Li and Cheng (1999) utilized the Geographical Information System (GIS) technique and established the Gaussian distribution function to model and predict the distribution of permafrost on the QTP. Nan et al. (2005) developed a numerical model to predict future changes of permafrost distribution on the QTP under climatic warming scenarios. Pang et al. (2009) used a model based on Kudryavtsev's formula to study the distribution and potential changes of ALT on the QTP. Cheng et al. (2012) used data from DEM, mean annual air temperature (MAAT), and the vertical lapse rate of air temperature for simulating decadal changes of permafrost on the QTP over the past 50 years. Guo et al. (2012) examined the current distribution and future change of permafrost on the QTP using the Community Land Model version 4 (CLM4) with an explicit treatment of frozen soil processes. To some extent, these studies satisfactorily simulated and predicted spatial and temporal distribution of permafrost and active layer thickness.

Here we try to introduce another model, the Geophysical Institute Permafrost Lab (GIPL) model, to simulate spatiotemporal variations of the ALT and TTOP in a scale of 1:500000 in the Source Areas of the Yellow River (SAYR). The GIPL model has been widely and efficiently applied in Alaskan and Russian arctic and sub-arctic regions (e.g., Sazonova and Romanovsky, 2003, 2004). The results of the model could help study the mechanisms of changes on cold environments, such as hydrological cycles, land desertification, and evolutionary processes of vegetation and land use related to the processes and changes of the active layer and near-surface permafrost in the SAYR.

The GIPL model based on Kudryatsev's equation and its modified versions have received substantial attention from geocryologists and cold regions engineers since they have effectively accounted for the thermal effects of vegetation cover, snow cover, soil properties, and regional climate variations (Romanovsky and Osterkamp, 1997; Sazonova and Romanovsky, 2003; Pang et al., 2009). The rapid development and extensive applications of GIS techniques and spatial analysis have facilitated the treatment and visualization of input data and output products (Anisimov et al., 1997; Shiklomanov and Nelson, 1999; Pang et al., 2009). Particular efforts were made with GIS techniques to downscale monthly air temperature derived from CRU TS3.0 dataset, to incorporate snow depth derived from passive remote sensing data of SMMR and SSM/I, vegetation type, soil properties and other parameters together, and to interpolate and visualize the model output products in a GIS environment.

1 Materials and methodologies

1.1 Permafrost in the SAYR

The SAYR (between 33°42.4′–35°29.0′N and 95°53.5′–98°49.4′E) on the northeastern QTP occupies the Yellow River valley above Duoshixia with a total catchment area of approximately 2.9×10^4 km^2 (Luo et al., 2011) (Figure 1).

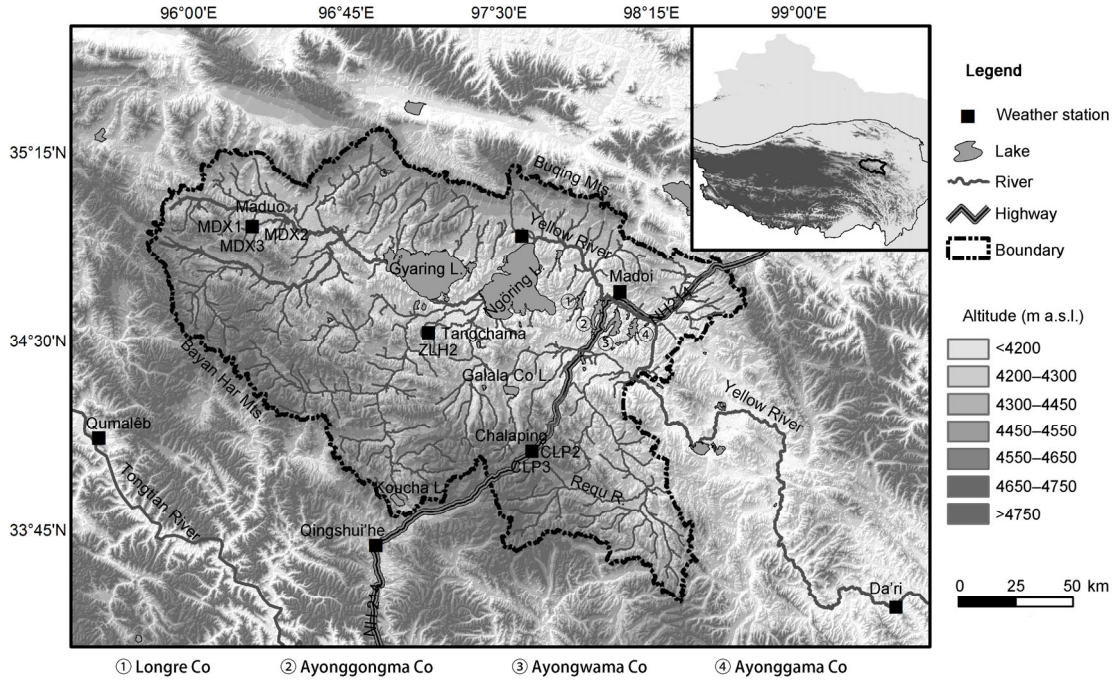

Figure 1 Geography of the Source Areas of the Yellow River (SAYR) on the northeastern QTP.

4491 m a.s.l. The spatial pattern of permafrost in the SAYR consists of a mosaic of continuous, discontinuous, and sporadic permafrost and seasonal frozen ground (Jin et al., 2009). Permafrost is obviously controlled by elevation and geomorphology. According to field investigations and ground temperature records, permafrost thickness is less than 100 m and is generally warm (>−1°C), with some exceptions on very high mountain tops (Luo et al., 2012a). Areal continuity of permafrost tends to increase with rising elevations towards the Buqing Mountains in the north and the Bayan Har Mountains in the south. The lower limit of permafrost is 4420 m a.s.l. on the north (shadowy) slopes of the Bayan Har Mountains, and 4350 m a.s.l. on the south (sunny) slopes of the Buqing Mountains (Jin et al., 2009; Luo et al., 2012b). Seasonally frozen ground or talik occurs primarily at regions below 4350 m a.s.l., such as in the peripheries of the Sisters Lakes (the Gyaring and Ngöring lakes), major river valleys, bare or open ground with little vegetation coverage, and in the southeastern SAYR. As revealed by borehole drilling and temperature records in 2010–2012, the lowest MAGT is −1.8°C and the thickest permafrost is 75 m. Both were found at an elevation of about 4720 m a.s.l. at Chalaping close to the Bayan Har Mountain Pass along the National Highway G214 (Luo et al., 2012a).

1.2 Descriptions of the GIPL model

The GIPL model includes two parts: the approximate computational solutions and the GIS approach that allows visual display and analysis on the spatial distribution of various model input and output of geographical parameters. As for the computational solutions, it calculates ALT and TTOP by treating the ground as a homogenous thermal conductivity body with different thermal properties in the frozen and thawed states, and estimating the impacts of thermal effects of vegetative and snow covers. Due to the minimal contribution to local variations in the ALT and TTOP, the effects of geothermal heat flux are ignored. Air temperature is regarded as the most important upper boundary condition for the ALT and TTOP. The daily surface (ground or vegetation surface during the summer and snow surface during the winter) temperature is assumed to behave in accordance with:

$$T(t) = T_{\mathrm{a}} + A_{\mathrm{a}} \sin\left(\frac{2\pi}{\tau} t\right), \tag{1}$$

where T_{a} and A_{a} are respectively the MAAT and its annual amplitude, τ is the period of temperature cycle (one year), and t is the time. The computational solutions for calculating the depth of seasonal freezing or thawing are as follow:

$$Z = \frac{2\left(A_{\mathrm{gs}} - \left|\overline{T_{\mathrm{ps}}}\right|\right)\sqrt{\lambda \cdot \tau \cdot \frac{C}{\pi}} + \frac{(2A_z \cdot C \cdot Z_c + \rho L \cdot Z_c) \cdot \rho L \sqrt{\lambda \cdot \tau / (\pi \cdot C)}}{2A_z \cdot C \cdot Z_c + \rho L \cdot Z + (2A_z \cdot C + \rho L) \cdot \sqrt{\lambda \cdot \tau / (\pi \cdot C)}}}{2A_z \cdot C + \rho L}, \tag{2}$$

where

$$A_z = \frac{A_{gs} - \left|\overline{T_{ps}}\right|}{\ln\left(\frac{A_s + \rho L / 2C}{\overline{T_{ps}} + \rho L / 2C}\right)} - \frac{\rho L}{2C}, \quad (3)$$

$$Z_c = \frac{2\left(A_{gs} - \left|\overline{T_{ps}}\right|\right)\left(\frac{\lambda \cdot \tau \cdot C}{\pi}\right)^{1/2}}{2A_z \cdot C + \rho L}, \quad (4)$$

where Z is the maximum depth (m) of seasonal frost or thaw, A_{gs} is the amplitude of annual periodic ground surface temperature, T_{ps} is the mean annual temperature at the bottom of seasonal freezing or thawing depth. λ and C are thermal conductivity and volumetric heat capacity of the soil (W m^{-1} °C^{-1} and J m^{-3} °C^{-1}), respectively. ρ is the dry bulk density of the soil (kg m^{-3}) and L is the volumetric latent heat of the water fusion in the ground (J m^{-3}).

Seasonal variations of ground surface temperature can be expressed by the harmonic function similar to eq. (1). Then mean annual temperature at seasonal freezing or thawing depth can be estimated by the eq (5):

$$T_{ps} = \frac{0.5T_{gs}\left(\lambda_f + \lambda_t\right) + A_{gs}\frac{\lambda_t - \lambda_f}{\pi} \times \left[\frac{T_{gs}}{A_{gs}}\arcsin\frac{T_{gs}}{A_{gs}} + \sqrt{1 - \frac{T_{gs}^2}{A_{gs}^2}}\right]}{\lambda^*}, \quad (5)$$

$$\lambda^* = \begin{cases} \lambda_f, & \text{if numerator} < 0, \\ \lambda_t, & \text{if numerator} > 0, \end{cases} \quad (6)$$

where λ_f and λ_t are thermal conductivities of frozen ground and thawed ground (W m^{-1} °C^{-1}), respectively, and T_{gs} is the mean annual temperature (°C) at the ground surface. As for the regions with permafrost, T_{ps} is the mean annual temperature (°C) at permafrost table. Where the regions with seasonally frozen ground (absent of pemafrost), T_{ps} is the mean annual temperature (°C) at the bottom of seasonal freezing layer.

All the input parameters are listed in Table 1.

The GIPL model regards the complex systems of air, surface vegetation, snow cover, and active layer as a set of individual layers; each layer with different thermal properties. However, the scheme is not totally additive, as the introduction of thermal effects of a new layer already includes the thermal effects of all the layers above it.

The thermal impacts of surface vegetation on the active layer differ with vegetative type and coverage (Zhou et al., 2000). Surface vegetation usually acts as an insulator that keeps the heat on the ground surface in the wintertime and warms the ground for the whole summer period. The total effect of these two influences is dependent on duration of summer and winter seasons, continentality of climate, and other local factors. The mean annual temperatures on ground surface are warmer than the near-surface, which will eventually result in an increase of TTOP.

Table 1 Input variables and parameters

Input variables	Notation
Annual amplitude of air temperate	A_a (°C)
Mean annual air temperature	T_a (°C)
Annual amplitude of the ground surface temperature	A_{gs} (°C)
Mean annual surface temperature	T_{gs} (°C)
Mean annual temperature at the bottom of active layer	T_{ps} (°C)
Volumetric latent heat	L (J kg$^{-1)}$
Thermal conductivity of snow	λ_{sn} (W m^{-1} °C^{-1})
Thermal conductivity of frozen ground	λ_f (W m^{-1} °C^{-1})
Thermal conductivity of thawed ground	λ_t (W m^{-1} °C^{-1})
Volumetric water content	W_{vol} (fraction of 1)
Volumetric heat capacity of snow cover	C_{sn} (J kg^{-1} °C^{-1})
Volumetric heat capacity of soil skeleton	C (J kg^{-1} °C^{-1})
Density of soil skeleton	ρ (kg m^{-3})
Volumetric heat capacity of frozen ground	C_f (J kg^{-1} °C^{-1})
Volumetric heat capacity of thawed ground	C_t (J kg^{-1} °C^{-1})

On the QTP, the high vegetation coverage lowers the ground temperatures and reduces the seasonal thaw depth (Zhou et al., 2000; Jin et al., 2008). Additionally, the onset of ground thawing and freezing processes at sites with higher vegetation coverage on the QTP are latter than those with lower coverage where greater variability in ground temperatures and more sensitive changes in air temperature are observed. Snow cover is of great importance in heat exchange between ground surface and the atmosphere. The late-spring residual snow cover (snowpack) on ground surface delays seasonal thawing even if the air temperature rises above freezing in spring. While at summertime, surface vegetation cover reduces solar radiation from penetrating into the ground and warming it (Sazonova and Romanovsky, 2003). After calculating the thermal effects of vegetation and snow covers, the mean annual temperature and seasonal amplitude of temperature variations on ground surfaces are:

$$T_{vg}=T_a+\Delta T_{sn}, \text{ and } A_{vg}=A_a-\Delta A_{sn}, \quad (7)$$

$$T_{gs}=T_{vg}+\Delta T_v, \text{ and } A_{gs}=A_{vg}-\Delta A_v, \quad (8)$$

ΔT_{sn}, ΔT_v, ΔA_v, ΔA_{sn} are adjustments for the thermal effects of snow cover and vegetation cover, respectively. Further descriptions of the model could be found in the papers of Romanovsky and Osterkamp (1997) and Sazonova and Romanovsky (2003).

1.3 Data source

The SAYR is divided into 1170 sub-grids at a scale of 0.05° (approximately 5 km). Then the values of elevation, longitude, and latitude are combined into one single shape file

through extracting from the SRTM DEM data in ArcGIS. Most input data (excluding monthly air temperature) are from "Environmental and Ecological Science Data Center for West China, National Natural Science Foundations of China" (http://westdc.westgis.ac.cn). Snow depth datasets are originally generated from the brightness temperature data derived from SMMR and DMSP SSM/I radiances with a spatial resolution of 25 km×25 km (Che et al., 2008). In this study, each sub-grid is assigned with snow depth data from the original 25 km×25 km grid which the sub-grid point falls into. The applicability is verified by correlation analysis between the snow depth from remote sensing and measurements at the Madoi Meteorological Station (Figure 2).

Most vegetation type data used in this study are derived from Vegetation Maps of China in scale of 1∶1000000 (http://westdc.westgis.ac.cn); some vegetation type data are from field investigations. Thermal properties of soils are assigned to each type of vegetation. The data of soil textures, dry bulk density and soil moisture content are partially from the field investigations in 2009–2012, and most are from the multi-layer soil particle-size distribution dataset in China in scale of 1∶1000000 (Wei et al., 2012). The thermal properties of frozen and thawed soils are estimated proportional to their textures, dry bulk density and soil moisture content by referring to empirical values according to Xu et al. (2010). Since there is only one long-term meteorological station (Madoi) in the SAYR, the GIS techniques are implemented to downscale monthly air temperature from the CRU TS3.0 datasets into 0.05°×0.05° sub-grid point. To keep time consistency with the snow depth data starting from 1980, the original data for monthly air temperature from the CRU TS3.0 datasets are on a scale of 0.5° and in a time series from 1980 to 2006. They are produced on the basis of the archived data of monthly mean air temperatures interpolated from more than 4000 weather stations distributed around the world (Mitchell and Jones, 2005). The region with interpolated data in the vicinity of the SAYR in this study has more than 80 grid points for the CRU TS3.0 datasets. A combination of the ordinary Kriging method with correction of elevational effect by using vertical lapse rate of air temperature are applied in processing the original CRU TS3.0 datasets (Li et al., 2005):

$$z(x_i) = z(x_i)' + (h_i - h_M) \times v / 100, \quad (9)$$

where h_i and h_M are the elevation of predicting grid points and the elevation of referencing grid points, respectively, and v is the vertical lapse rate of air temperature, which are used for different latitudinal and altitudinal zones on the QTP (Xie and Zeng, 1983). The elevation of 0.05° sub-grid points derived from the SRTM DEM data is used as co-variables. Then, the cross-variogram is established on the basis of the temperature-elevation relationship at these interpolated grid points. The accuracy of the data interpolated from the CRU TS3.0 datasets is evaluated by air temperature records from long-term meteorological stations at Da'ri, Madoi, Qingshui'he and Qumalai (Figure 1). The correlation coefficients of the air temperatures between the interpolated and measured values are 0.99, 0.99, 0.98, and 0.96 for the abovementioned four stations, respectively (Figure 3). Therefore, the interpolated results can be used as the input parameters for the GIPL model.

2 Results

2.1 Model validation

The GIS is applied to store and visualize input parameters such as air temperature, snow depth, vegetation types, and soil properties. After data processing and parameterization of input variables, the calculation routines are called in with necessary parameters for computing of the ALT and TTOP

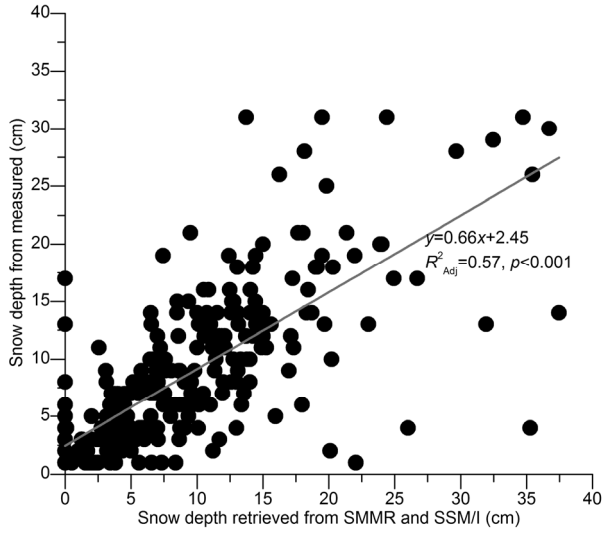

Figure 2 Correlation of snow depth between remote sensing data and the Madoi Station.

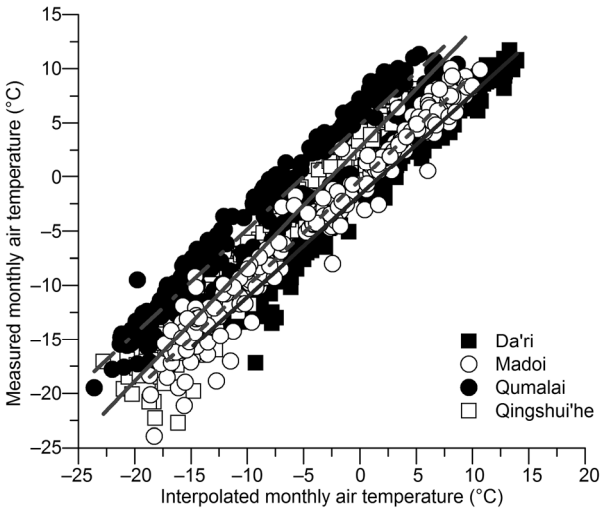

Figure 3 Correlation of monthly air temperature among the data interpolated from CRU TS3.0 datasets and measured values at the Da'ri, Madoi, Qingshui'he, and Qumalai meteorological stations.

values. The ALT and TTOP values from eight field monitoring sites (CLP2, CLP3, ELH1, ELH2, ZLH1, MDX1, MDX2, and MDX3) in the SAYR are used to evaluate the performance of the model (Figure 1). Thermal and physical properties of soils for these selected sites were obtained by laboratory measurements of soil samples from field work (Table 2). The calculated and measured ALT values are compared in Figure 4(a) and 4(b). Modeled results of ALT and TTOP values with interpolated data for soil temperatures at the Madoi Meteorological Station are checked in Figure 4(c) and 4(d). The relative deviations between the modeled results and measured values for the eight sites and the Madoi Meteorological station are less than 36% and 31%; typically, they are within 20%.

2.2 Distribution and changes of the ALT and TTOP in the SAYR

The spatial distribution and dynamics of the calculated ALT and TTOP values in the SAYR are shown in Figures 5 and 6. Based on simulations of the GIPL model, spatial distribution of ALT and TTOP in the SAYR had changed dramatically under a warming climate from 1980 to 2006.

Since air temperature decreases with altitude, the mean annual temperature of the ground is also reduced, which leads to reduced thickness of seasonally thawing layer and

Table 2 Thermophysical properties of the soils at selected sites and the Madoi Meteorological Station in the SAYR

Sites	Soil types	W_{vol} (%)	ρ(kg m^{-3})	λ_f (W m^{-1} °C^{-1})	λ_t (W m^{-1} °C^{-1})
CLP2	peaty clay	88	950	2.12	1. 63
CLP3	loam	67	1060	1.78	1.22
ZLH2	loam	32	1380	1.69	1.05
MDX1	clayey sand	25	1520	1.62	1.17
MDX2	clayey sand	23	1560	1.47	1.03
MDX3	clayey sand	27	1570	1.86	1.25
ELH1	gravel and sand	15	1330	0.86	0.58
Madoi	gravel and sand	12	1290	0.74	0.52

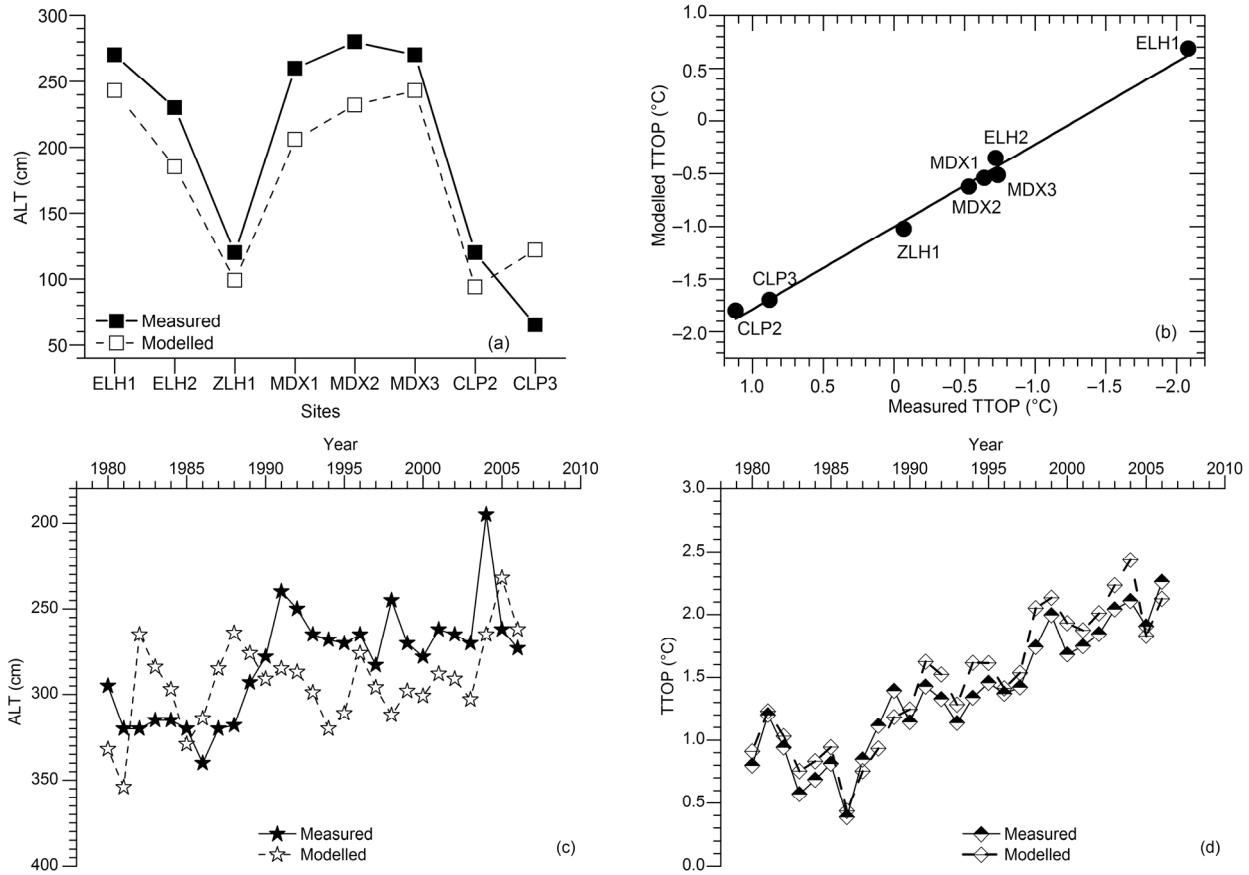

Figure 4 Validation of modeling results at the eight field sites ((a) for ALT and (b) for TTOP) and the Madoi Meteorological Station ((c) for ALT and (d) for TTOP) in the SAYR.

increased thickness of frozen layer. The ALT values, both measured and calculated, display a vertical zonation in the SAYR, i.e., the ALT declines with a rising elevation, during the period from 2010–2012 (Luo et al., 2013). The ALT is greater than 3.0 m at most sites in the Reqü River watershed in the southeastern SAYR, which is dominated by seasonally frozen ground and with elevation generally less than 4300 m a.s.l. In the Reqü River watershed, there are some exceptions at mountain tops near the water divide of the SAYR. The ALT values are generally less than 1.5 m at the southwestern SAYR and on the northern slopes of the Bayan Har Mountains, generally higher than 4500 m a.s.l. As for the Buqing Mountains in the northern SAYR with elevations from 4400 to 4700 m a.s.l., the ALT is generally between 1.0 and 2.0 m (Figure 5).

The model results demonstrate that permafrost in the SAYR is warm, thermally unstable, and very sensitive to climate warming and anthropogenic disturbances. This also matches the field investigations in 2010–2012 (Luo et al., 2012a, 2013). The spatial distribution of the TTOP in the SAYR simulated by the GIPL model also indicates an evident elevational zonation. The TTOP rises with decreasing elevation from the northern and southern parts towards the central and southeastern parts of the SAYR. The positive TTOP values indicate that the distribution of seasonally frozen ground is mainly in the central and southeastern parts of the SAYR, such as in the peripheries of the Gyaring and Ngöring lakes, on watersheds of the Longre Co, the Ayonggongma Co, the Ayongwama Co, and the Ayonggama Co lakes in the neighborhood of Madoi county town,

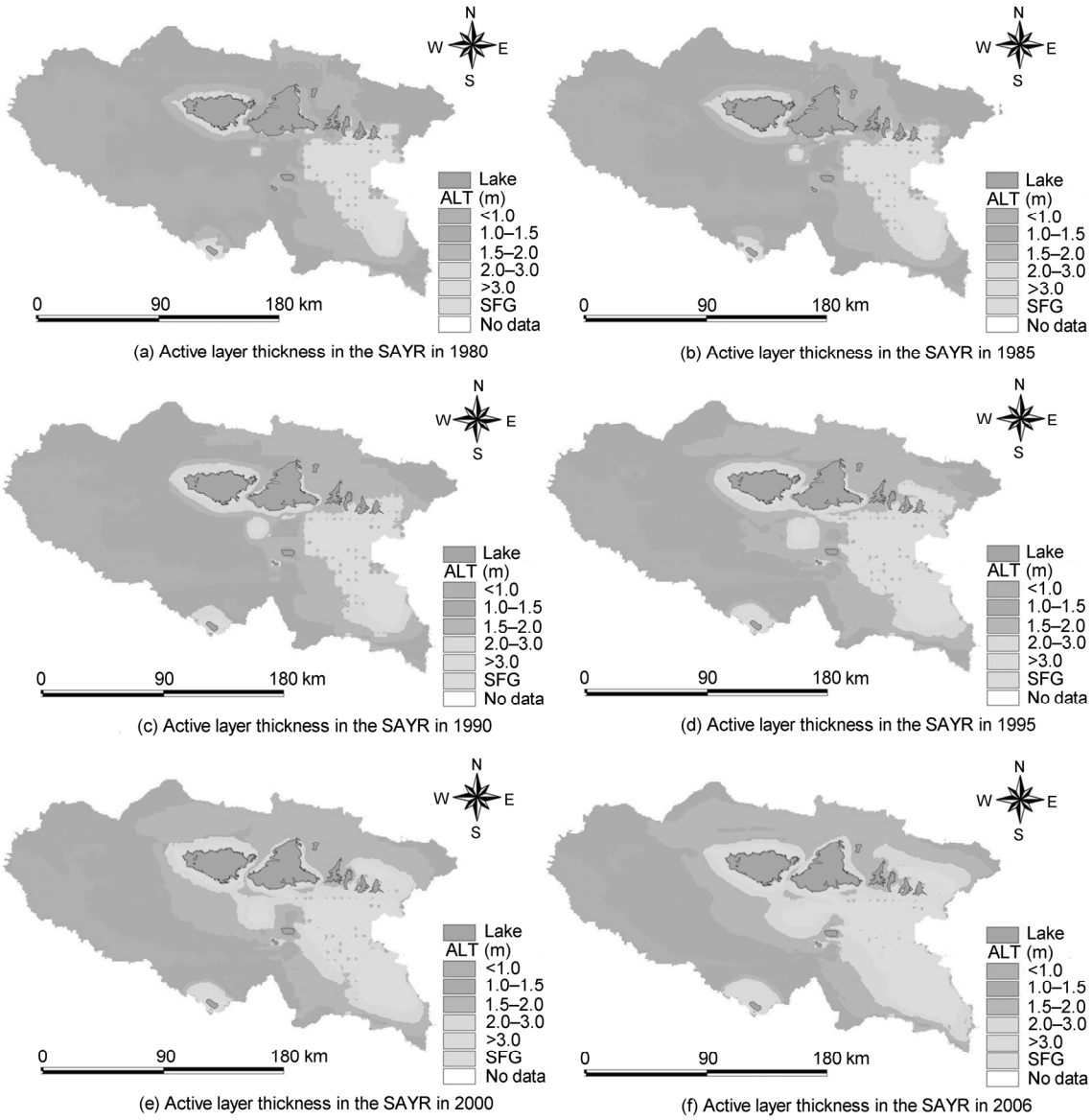

Figure 5 Changes in spatial distribution of the active layer thickness (ALT) in the SAYR during the period 1980–2006 (SFG denotes seasonally frozen ground).

the Koucha Lake on the southern part of the SAYR, and the valleys of the mail river and major tributaries of the Yellow River. The elevations of these regions are generally less than 4350 m a.s.l. Those regions with the lowest TTOP (less than –1.5°C) are distributed primarily on the southwestern and northern parts of the SAYR, such as the northern flanks of the Bayan Har Mountains and the southern flanks of the Buqing Mountains. Regions of TTOP less than –2°C appear only at some mountain tops that have an elevation greater than 4700 m a.s.l. As revealed by temperature measurements from the boreholes drilled in 2010, the soil temperature at depths of 10–15 m (where the temperature usually varied less than 0.1°C in a typical year) are –1.8°C at Chalaping (34°15′N, 97°51′E; 4720 m) and –0.22°C at Yeniugou (34°24′N, 97°57′E; 4420 m) (Luo et al., 2012a). The region with TTOP between –1 and 0°C appeared in the rest of the SAYR, such as the southern part to the south of the Gyaring Lake and in the western part of the SAYR.

The ALT and TTOP in the SAYR respond positively to climate changes and human disturbances. Climate warming has been prominent on the QTP since the 1980s (Cai et al., 2003), and much more pronounced in the source areas of the Yangtze, Yellow, and Lancang-Mekong rivers where the increasing rate of air temperature has been accelerating since the late 1990s, especially after 2001 (Yi et al., 2011). The ground surface temperature is closely related to the ALT and TTOP increasing at an average rate of 0.06°C yr^{-1} over the period 1980–2007 on the QTP (Wu and Zhang, 2010). The trends of changes in the ALT and TTOP in the SAYR during 1980–2006 are consistent with the climate warming trends. Based on the GIPL model, the mean ALT of the entire SAYR increased from 1.8 m in 1980 to 2.4 m in 2006, at an average rate of 2.2 cm yr^{-1}; the rate was

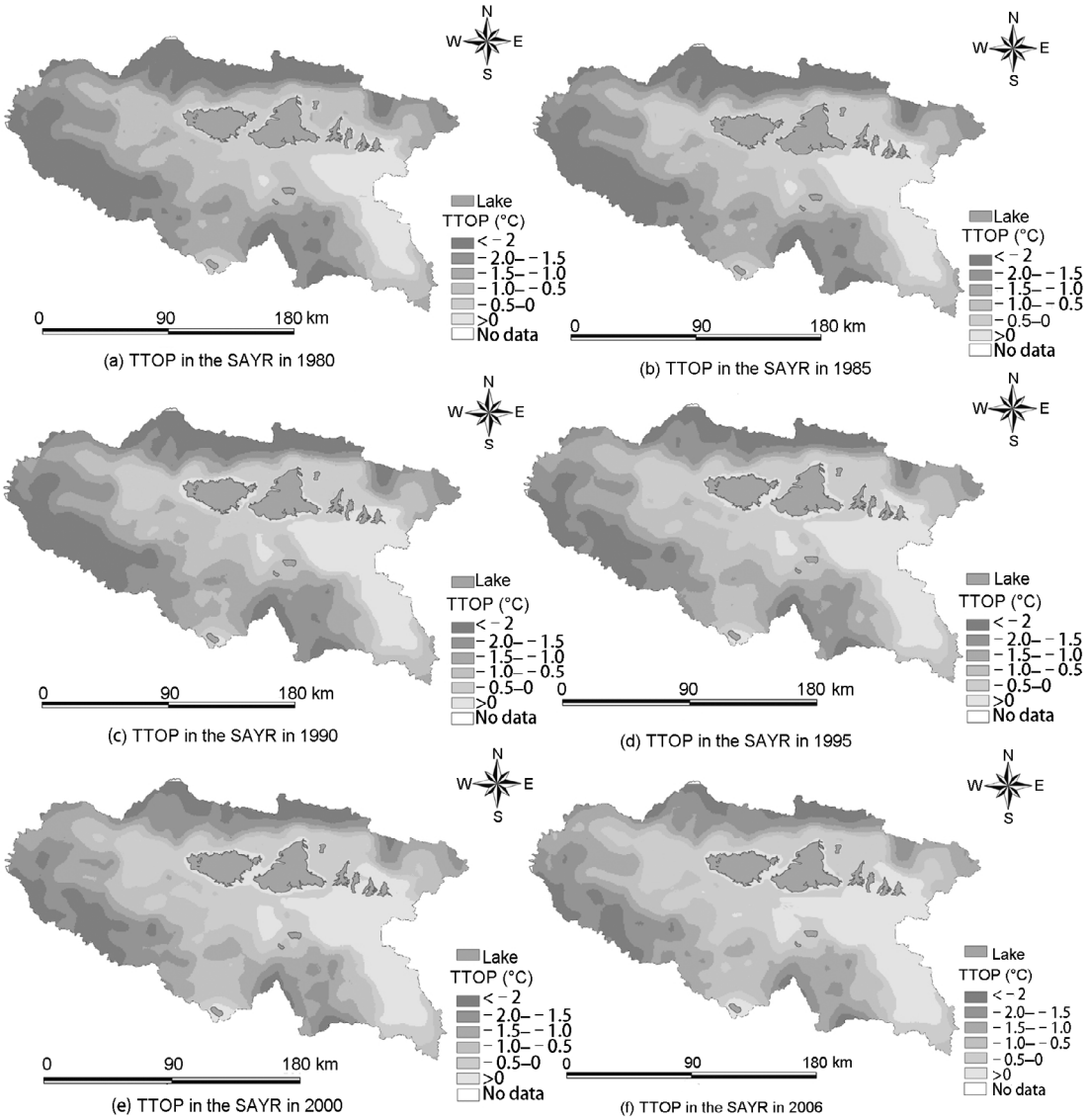

Figure 6 Distribution and changes of TTOPs in the SAYR.

accelerated to 4.3 cm yr^{-1} between 2000 and 2006. On the other hand, the minimum ALT changed from 0.45 m in 1980 to 0.7 m in 2006, with an average rate of 0.93 cm yr^{-1}, slower than those of the total mean ALT (Figure 7(a)). As modeled by the GIPL model, the average TTOP in the SAYR increased from –1.1°C in 1980 to –0.6°C in 2006, with an average rate of 0.018°C yr^{-1}. During the same period, the corresponding minimum TTOP of the SAYR increased from –3.4°C in 1980 to –3.1°C in 2006 at an average rate of 0.011°C yr^{-1}, slightly smaller than the increasing rate of mean TTOP in the SAYR (Figure 7(b)).

As shown by the GIPL model, the permafrost regions in the SAYR with minimum ALT and TTOP values are comparatively thermally stable. The changing trends of ALT in warm permafrost regions are much slower than in cold permafrost regions, while change trends of TTOP behave the opposite way. Studies by Wu et al. (2010) showed that the average increasing rate of ALT is approximately 5.0 cm yr^{-1} in cold permafrost regions and 11.2 cm yr^{-1} over warm permafrost areas with anthropogenic disturbances along the QTEC in the Interior of the QTP. The monitoring network of increasing rate of ALT from Li et al. (2012) has demonstrated the same pattern of spatial variations of ALT on the QTP. These two studies correspond to spatial difference of changing rates of ALT in the SAYR as modeled by the GIPL model.

2.3 Changes of permafrost

The degradation of permafrost is closely related to the increase of TTOP. Taken by the raster calculation under an ArcGIS environment, the areal extent of the regions with subzero TTOP was calculated using the GIPL model. The total areal extent with a subzero TTOP decreased from approximately 2.4×10^4 km^2 in 1980 to 2.2×10^4 km^2 in 2006, at a rate of 74 km^2 yr^{-1} (Figure 8). Seasonally frozen ground is located mainly in the south-central SAYR where permafrost degraded northwards to the Buqing Mountains and southwards to the Bayan Har Mountains as evidenced by the GIPL model. The areas with degrading permafrost also include the regions surrounding the Koucha Lake in the southwestern SAYR with an elevation generally above 4500 m (Figure 6). Figure 6(a), 6(b) and 6(c) show that surrounding regions of the Koucha Lake have subzero TTOP values before the 1990s, but permafrost gradually changed to seasonally frozen ground in the 2000s (Figure 6(d), 6(e) and 6(f)). As for the basins with sparse vegetation south of the Sisters (Gyaring and Ngöring) Lakes and the river valleys in the eastern SAYR, the widespread distribution of seasonally frozen ground, i.e., areas with above zero TTOP from the results of the model, is also verified by field investigations.

3 Discussions

Distribution and change of ALT in part or the entire QTP have been studied previously based on permafrost models (Pang et al., 2009; Wu and Zhang, 2010; Guo et al., 2012), but the changes and distribution of TTOP, an indicator of the occurrence of permafrost, were occasionally discussed with some limited monitoring data along the QTEC and NH 214. The trends of ALT changes in the SAYR between 1980 and 2006 in this study agree well with trends of ALT changes in 1980–2001 simulated by one-dimensional heat transfer model with phase change (Oelke and Zhang, 2007), as well as trends of ALT changes in 1980–2010 modeled by CLM4 (Guo et al., 2012). With TTOP persistently rising

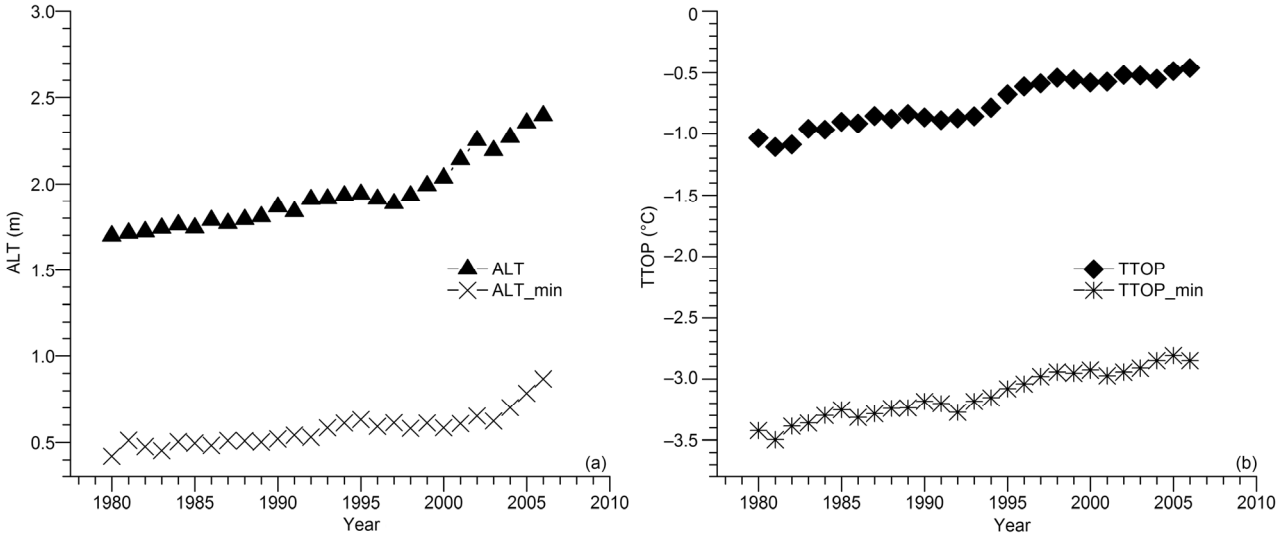

Figure 7 Changes of average ALT and TTOP of the SAYR in 1980–2006. The product sign in (a) represents the minimum value of ALTs, and the asterisk sign in (b) represents the minimum value of TTOP.

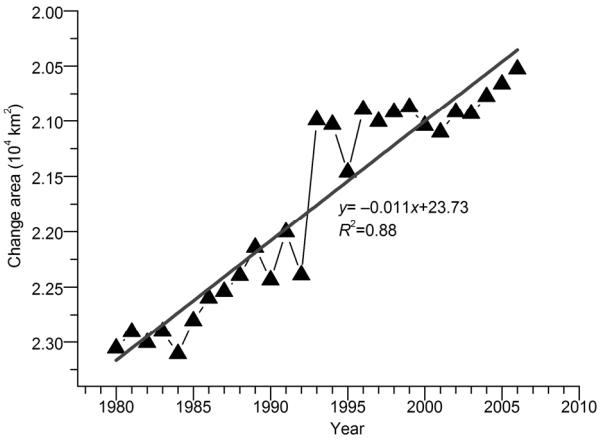

Figure 8 Change in the areal extent of regions with subzero TTOP in the SAYR.

and eventually approaching the melting point of ice (usually close to 0°C) under a warming climate, the ground ice near the permafrost surface may melt, and ground surface and soils at shallow (<50 cm) depths would tend to dry up as a combined result of deepening seasonal thaw depth and lowering suprapermafrost water table. Consequently, alpine meadows may be adversely affected by water shortage (Liang et al., 2007). Therefore, the distribution and change of soil moisture and temperatures in the active layer in the SAYR play very important roles in studying the plant ecology, permafrost hydrology, land desertification, and stability of cold regions engineering foundations. Based on the applications of the GIS-aided GIPL model, the spatiotemporal distribution of ALT and TTOP in the SAYR was modeled in this study.

The occurrence and dynamics of permafrost are controlled mainly by heat balance between the atmosphere and ground. Local factors, such as surface canopies (vegetation and snow covers), organic-layer thickness, topography, hydrology, geothermal fluxes, and thermal properties of soils, are also important for the thermal state of the active layer and permafrost (Wu et al., 2010). Compared with other factors, snow and vegetation are the most important ones influencing the distribution and dynamics of the active layer and permafrost. The removal of vegetation will heat the ground and result in the rising of TTOPs and increasing of ALTs, hence it is very important to study changes of vegetation cover and the land-use and land-cover changes in the SAYR. Snow cover can greatly impact the surface and thermal offsets among the air, ground surface and subsurface (Smith and Riseborough, 2002). Therefore, the regions with similar MAATs may have diverse ground surface temperatures and TTOP. Additionally, the influences of snow cover on the thermal regime of active layer differ in snow depth and seasonality. For example, the delaying of snow cover onset and the snow cover disappearance date can result in lowered ground temperatures and shallower thaw depths, whereas the earlier disappearance of snow cover can raise the ground temperature and deepen thaw depths (Ling and Zhang, 2003). Although snow cover prevails on the QTP from September to the next May, snow depths are much shallower than in most arctic and subarctic regions (Ma and Qin, 2012). Furthermore, snow cover is very unstable due to the stronger plateau radiation and warmer climate. Field investigations and experiments should be carried out to quantitatively study the influence of snow on the thermal regimes of the active layer and permafrost soils on the QTP.

There are several issues related to deviations of the performance of the GIPL model. Potential errors exhibited in data processing may introduce greater uncertainties in modeling spatial distribution of ALT and TTOP in the SAYR. Due to coarse spatial resolutions of the data for air temperature, snow depth, vegetation and soil properties, the thermal effects of local factors and climate warming could not be fully accounted for, although the air temperature had been downscaled into a resolution of 5 km. The CRU TS3.0 datasets were originally downscaled based on the statistical relationships and interpolations of air temperature from a large quantity of meteorological stations worldwide, hence the repeated downscaling processes may bring in new errors. As a result of insufficient field work, an additional reason that may affect the model's performance is that some parameters of the model are presumptive, and they cannot be validated by on-site measurements. The accuracies of input data most models confront during the processing therefore should be improved to further improve the GIPL model.

Additionally, more precise snow depth data may be needed to get better results, since the spatial heterogeneity of snow depth varied enormously. For example, no significant correlation was found at a distance larger than 100 m in Barrow, Alaska (Shiklomanov et al., 2010). Nevertheless, several selected sites had convincing results to support the GIPL model. Moreover, the interpolated ALT and TTOP from soil temperature measurements at the Madoi Meteorological Station also demonstrated the increase trend in the active layer thickness and temperature during the period of 1980–2006 (Luo et al., 2012b), which is consistent with changing rates predicted by the GIPL model. The shallower thickness of snow packs (less than 20 cm) on the QTP tends to reduce the ground temperature and increase the seasonal freezing depth (Zhou et al., 2013). Hence, in the future more work should be done for the spatial difference among ALT and TTOP and their influencing factors such as organic soil layer, snow depth, and microtopography.

The predicted increases of ALT in the SAYR by the GIPL model are more prominent than those along the Qinghai-Tibet Highway. This may be related to regional differentiations of plateau climate warming. Increasing air temperature is more prominent in the SAYR than in the Interior of the QTP (Yi et al., 2011). Active layer is the buffer layer between the atmosphere and permafrost, and is directly affected by increasing air temperature. The correlation

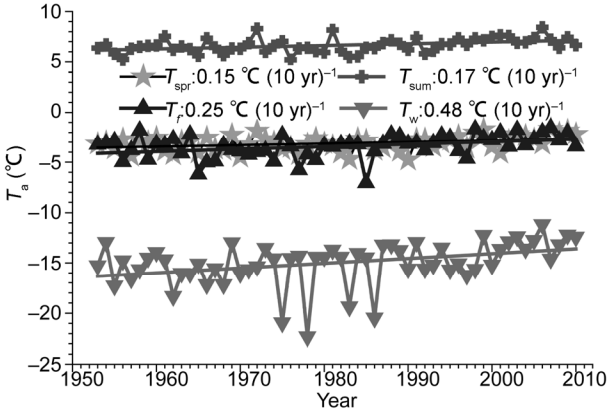

Figure 9 Change trends of air temperature in spring (T_{spr}), summer (T_{sum}), autumn (T_f), and winter (T_w) in the Madoi Station.

analysis between variations of ALT and increasing air temperature has demonstrated that warming in air temperature, especially in winter temperature, has an important effect on the variation of ALT along the QTEC (Li et al., 2012). In addition, Figure 9 shows that increases in air temperatures in the Madoi Meteorological Station in spring, summer, autumn and winter are 0.15, 0.17, 0.25, and 0.48°C (10 yr)$^{-1}$, respectively, which are greater than those along the Qinghai-Tibet Highway. Therefore, the variations of ALT are probably more significant in the SAYR during the same period.

4 Conclusions

The depth of seasonal freezing and thawing and mean annual temperature at the bottom of the active layer in the SAYR in 1980–2006 were studied based on the GIPL Model. Monthly air temperature, monthly snow depth, vegetation type, and soil properties were taken as input data of the model after handling in ArcGIS. The GIPL model takes elevational zonation into full account by incorporating it into monthly air temperature during the downscaling processes. Measured data from eight field sites during 2010–2012 were used to validate the model. Model results show that variations of ALT and TTOP in the SAYR are affected by local factors, such as slope aspects and angles, surface vegetation, soil types, and hydrology. The elevation controls spatial differentiation of ALT and TTOP. The higher the elevation, the lower the TTOP, and the shallower the ALT.

On account of rising air temperature in the past two decades, the average seasonal thawing depth has increased significantly, and the average TTOP has dramatically risen in the SAYR. As studied by the GIPL model, the average ALT in the SAYR increased from 1.8 m in 1980 to 2.4 m in 2006 at an average rate of 2.2 cm yr^{-1}, faster than those monitored results along the QTEC. The average TTOP in the SAYR increased from –1.1°C in 1980 to –0.6°C in 2006, at an average rate of 0.018°C yr^{-1}. Furthermore, ALT and TTOP have increased since the 2000s. The remarkable changes of TTOP have resulted in an areal decline in the regions with subzero TTOP. According to the calculations in ArcGIS, in 1980–2006, the areas with subzero TTOP shrank from 2.4 × 10^4 to 2.2 ×10^4 km^2 at an average rate of 74 km^2 yr^{-1}.

The model results need to be further validated using more monitoring data, and more detailed information and parameters such as vegetation type, soil properties, especially spatial differential scales of ALT and TTOP needs to be studied from field work. Furthermore, future climate change scenarios should be utilized to facilitate the understanding of changes and deterioration of cold regions environments.

This work was supported by the National Natural Science Foundation of China (Grant Nos. 41301068, 41121061), the State Key Laboratory of Frozen Soils Engineering (Grant No. Y252J41001,) and the Foundation for Excellent Youth Scholars of CAREERI, CAS (Grant No. 51Y351051). We thank two anonymous reviewers for their valuable comments and suggestions. We also thank the Environmental and Ecological Science Data Center for West China, the National Natural Science Foundation of China, which provided the data sets "Snow depth datasets of China (1978–2008) in scale of 25 km", "1 :1000000 soil map of China", "1 :1000000 vegetation map of China".

Anisimov O A, Shiklomanov N I, Nelson F E. 1997. Global warming and active-layer thickness: Results from transient general circulation models. Glob Planet Change, 15: 61–77

Cai Y, Li D L, Tang M C. 2003. Decadal temperature changes over Qinghai-Xizang Plateau in recent 50 years. Plateau Meterol, 22: 464–470

Che T, Li X, Jin R, et al. 2008. Snow depth derived from passive microwave remote-sensing data in China. Annals Glaciol, 49: 145–154

Cheng G D. 1984. Problems on zonation of high-elevation permafrost (in Chinese). Acta Geograph Sin, 39: 185–193

Cheng G D, Wu T H. 2007. Responses of permafrost to climate change and their environmental significance, Qinghai-Tibet Plateau. J Geophys Res, 112: F02S03

Cheng W M, Zhao S M, Zhou C H, et al. 2012. Simulation of the decadal permafrost distribution on the Qinghai-Tibet Plateau (China) over the past 50 years. Permafrost Periglac Process, 23: 292–300

Guglielmin M, Ellis C J E, Cannone N. 2008. Active layer thermal regime under different vegetation conditions in permafrost areas. A case study at Signy Island (Maritime Antarctica). Geoderma, 144: 73–85

Guo D L, Wang H J, Li D. 2012. A projection of permafrost degradation on the Tibetan Plateau during the 21st century. J Geophys Res, 117: D05106

Jin H J, Yu Q H, Wang S L, et al. 2008. Changes in permafrost environments along the Qinghai-Tibet engineering corridor induced by anthropogenic activities and climate warming. Cold Reg Sci Technol, 53: 317–333

Jin H J, He R X, Cheng G D, et al. 2009. Changes in frozen ground in the Source Area of the Yellow River on the Qinghai-Tibet Plateau, China, and their eco-environmental impacts. Environ Res Lett, 4: 1–11

King L, Herz T, Hartmann H, et al. 2006. The PACE monitoring strategy: A concept for permafrost research in Qinghai-Tibet. Quatern Int, 154–155: 149–157

Li R, Zhao L, Ding Y J, et al. 2012. Temporal and spatial variations of the active layer along the Qinghai-Tibet Highway in a permafrost region. Chin Sci Bull, 57: 4609–4616

Li X, Cheng G D. 1999. A GIS-aided response model of high altitude permafrost to global change, Sci China Ser D-Earth Sci, 42: 72–79

Li X, Cheng G D, Lu L. 2005. Spatial analysis of air temperature in the Qinghai-Tibet Plateau. Arctic Antarctic Alpine Res, 37: 246–252

Li X, Cheng G D, Jin H J, et al. 2008. Cryospheric change in China. Glob

Planet Change, 62: 210–218
Liang S H, Wan L, Li Z M, et al. 2007. The effect of permafrost on alpine vegetation in the source regions of the Yellow River (in Chinese). J Glaciol Geocryol, 29: 45–52
Ling F, Zhang T J. 2003. Impact of the timing and duration of seasonal snow cover on the active layer and permafrost in the Alaskan Arctic. Permafrost Periglac Process, 14: 141–150
Liu T L. 1983. A summarization of formulas of calculating frozen or melted depth abroad (in Chinese). J Glaciol Geocryol, 5: 85–95
Luo D L, Jin H J, Jin R, et al. 2011. The extraction of watershed characteristics of the Source Area of Yellow River based on SRTM DEM with ArcGIS, IEEE (in Chinese). IEEE Xplore: International Conference on Remote Sensing, Environment and Transportation Engineering (RSETE2011), Nanjing, China. doi: 10.1109/RSETE.2011.5964645
Luo D L, Jin H J, Lin L, et al. 2012a. New progress on permafrost temperature and thickness in the source area of the Huanghe River (in Chinese). Scient Geograph Sin, 32: 898–904
Luo D L, Jin H J, Lin L, et al. 2012b. Degradation of permafrost and cold-environments on the interior and eastern Qinghai Plateau (in Chinese). J Glaciol Geocryol, 34: 538–546
Luo D L, Jin H J, Lin L, et al. 2013. Distributive features and controlling factors of permafrost and the active layer thickness in the Bayan Har Mountains along the Qinghai-Kangding Highway on Northeastern Qinghai-Tibet Plateau (in Chinese). Scient Geograph Sin, 33: 635–640
Ma L J, Qin D H. 2012. Spatial-Temporal characteristics of observed key parameters for snow cover in China during 1957–2009 (in Chinese). J Glaciol Geocryol, 34: 1–11
Mitchell T D, Jones P D. 2005. An improved method of constructing a database of monthly climate observations and associated high-resolution grids. Int J Climatol, 25: 693–712
Nan Z T, Li S X, Cheng G D. 2005. Prediction of permafrost distribution on the Qinghai-Tibet Plateau in the next 50 and 100 years. Sci China Ser D-Earth Sci, 48: 797–804
Nelson F E, Outcalt S I. 1987. A computational method for prediction and regionalization of permafrost. Arct Alp Res, 19: 279–288
Oelke C, Zhang T J. 2007. Modeling the active-layer depth over the Tibetan Plateau. Arct Antarct Alp Res, 39: 714–722
Pang Q Q, Cheng G D, Li S X, et al. 2009. Active layer thickness calculation over the Qinghai-Tibet Plateau. Cold Reg Sci Technol, 57: 23–28
Riseborough D, Shiklomanov N, Etzelmüller B, et al. 2008. Recent advances in permafrost modelling. Permafrost Periglac Process, 19: 137–156
Romanovsky V E, Osterkamp T E. 1997. Thawing of the active layer on the Coastal Plain of the Alaskan Arctic. Permafrost Periglac Process, 8: 1–22
Sazonova T S, Romanovsky V E. 2003. A model for regional-scale estimation of temporal and spatial variability of active layer thickness and mean annual ground temperatures. Permafrost Periglac Process, 14: 125–139
Sazonova T S, Romanovsky V E. 2004. Permafrost dynamics in the 20th and 21st centuries along the East Siberian transect. J Geophys Res, 109: D01108
Shiklomanov N I, Nelson F E. 1999. Analytic representation of the active layer thickness field, Kuparuk River Basin, Alaska. Ecol Model, 123: 105–125
Shiklomanov N, Nelson F, Streletskiy D, et al. 2008. The Circumpolar Active Layer Monitoring (CALM) program: Data collection, management, and dissemination strategies. In: Kane D L, Hinkel K M, eds. Proc 9th Int Conf Permafrost, 2: 1–6
Shiklomanov N I, Streletskiy D A, Nelson F E, et al. 2010. Decadal variations of active-layer thickness in moisture-controlled landscapes, Barrow, Alaska. J Geophys Res, 115: G00I04
Wei S G, Dai Y J, Liu B Y, et al. 2012. A soil particle-size distribution dataset for regional land and climate modelling in China. Geoderma, 171–172: 85–91
Smith M W, Riseborough D W. 2002. Climate and the limits of permafrost: A zonal analysis. Permafrost Periglac Process, 13: 1–15
Streletskiy D A, Shiklomanov N I, Nelson F E. 2012. Spatial variability of permafrost active-layer thickness under contemporary and projected climate in Northern Alaska. Polar Geography, 35: 95–116
van Everdingen R O, ed. 2005. Multi-languge Glossary of Permafrost and Related Ground-ice Terms. Boulder: National Snow and Ice Data Center/World Data Center for Glaciology. 222
Wu Q B, Zhang T J. 2008. Recent permafrost warming on the Qinghai-Tibetan Plateau. J Geophys Res, 113: D13108
Wu J C, Sheng Y, Wu Q B, et al. 2010. Processes and modes of permafrost degradation on the Qinghai-Tibet Plateau. Sci China Earth Sci, 53: 150–158
Wu Q B, Zhang T J. 2010. Changes in active layer thickness over the Qinghai-Tibetan Plateau from 1995 to 2007. J Geophys Res, 115: D09107
Wu Q B, Zhang T J, Liu Y Z. 2012. Thermal state of the active layer and permafrost along the Qinghai-Xizang (Tibet) Railway from 2006 to 2010. Cryosphere, 6: 607–612
Xie Y, Zeng Q. 1983. Climatic conditions for the occurrence of permafrost in the Qinghai-Tibet Plateau (in Chinese). In: Proceedings of the Second National Conference on Permafrost. Lanzhou: Gansu People's Publishing House. 13–20
Xu X Z, Wang J C, Zhang L X. 2010. Physics of Frozen Soils (in Chinese). Beijing: Science Press. 84–90
Yi X S, Yin Y H, Li G S, et al. 2011. Temperature variation in recent 50 years in the three-river headwaters region of Qinghai Province (in Chinese). Acta Geograph Sin, 66: 1451–1465
Zhang T J. 2005. Spatial and temporal variability in active layer thickness over the Russian Arctic drainage basin. J Geophys Res, 110: D16101
Zhao L, Wu Q B, Marchenko S S, et al. 2010. Thermal state of permafrost and active layer in Central Asia during the international polar year. Permafrost Periglac Process, 21: 198–207
Zhou J, Kinzelbach W, Cheng G D, et al. 2013. Monitoring and modeling the influence of snow pack and organic soil on a permafrost active layer, Qinghai-Tibetan Plateau of China. Cold Region Sci Tech, 90–91: 38–52
Zhou Y W, Qiu G Q, Guo D X, et al. 2000. Frozen ground in China (in Chinese). Beijing: Science Press. 63–91